Journal of Sustainable Metallurgy (2018) 4:176–186
https://doi.org/10.1007/s40831-018-0173-5

INNOVATIONS IN WEEE RECYCLING

# Recycling Waste Crystalline Silicon Photovoltaic Modules by Electrostatic Separation

Pablo Dias[1,2] · Lucas Schmidt[1] · Lucas Bonan Gomes[3] · Andrea Bettanin[1] · Hugo Veit[1] · Andréa Moura Bernardes[1]

Published online: 14 March 2018


## Abstract

Photovoltaic (PV) modules contain both valuable and hazardous materials, which makes their recycling meaningful economically and environmentally. The recycling of the waste of PV modules is being studied and implemented in several countries. Current available recycling procedures include either the use of high-temperature processes, the use of leaching agents or a combination of both. In this study, waste of silicon-based PV modules are separated using an electrostatic separator after mechanical milling. An empirical study is used to verify if the separation works and to select and fix several parameters. Rotation speed of the roller and DC voltage are evaluated as a result of the separation of metals (silver and copper), silicon, glass, and polymers. The efficiency of metals' separation is determined by acid leaching of the corresponding fractions followed by inductively coupled plasma optical emission spectrometry (ICP-OES); that of polymer separation is determined by mass difference due to combustion of the corresponding fractions; and those of glass and silicon quantities are determined by X-ray diffraction (XRD) followed by characterization using Rietveld quantitative phase analysis (RQPA). It is shown that the optimal separation is obtained under different operating voltages of 24 and 28 kV and a rotation speed of 30 RPM or higher. Furthermore, it is shown that there is no significant difference among the tested parameters. Results provide a new option in the recycling of waste of silicon PV modules that can and should be optimized.

**Keywords** Crystalline silicon · Electrostatic separation · Material separation optimization · Recycling · Solar panel

## Introduction

### Waste Electric and Electronic Equipment (WEEE)

The demand for cleaner energy sources to overcome the use of fossil fuels and to slowdown climate change due to human activities creates a favorable scenario for photovoltaic technologies, which is considered a promising technology [1]. Photovoltaic (PV) modules are devices that can convert sunlight into electricity without any other source of energy; they can be made of numerous semiconductors materials [2]. However, PV modules have a technical lifespan of 20–30 years and will become electronic waste (WEEE) in the next few years, since the commencement of broad PV installation occurred in the 1990s [3]. End-of-life modules are expected to reach 5.5–6 million tons by the 2050s [4]. Therefore, it is essential to develop recycling technologies to reduce the amount of this

The contributing editor for this article was Bernd Friedrich.

**Electronic supplementary material** The online version of this article (https://doi.org/10.1007/s40831-018-0173-5) contains supplementary material, which is available to authorized users.

✉ Pablo Dias
pablo.dias@ufrgs.br

Andréa Moura Bernardes
amb@ufrgs.br

[1] Programa de Pós-Graduação em Engenharia de Minas, Metalúrgica e de Materiais (PPGE3M), Universidade Federal do Rio Grande do Sul (UFRGS), Av. Bento Gonçalves, 9500, Porto Alegre, RS 91509-900, Brazil

[2] Faculty of Science and Engineering, Macquarie University, Sydney, NSW 2109, Australia

[3] X-Ray Diffraction Laboratory, Geosciences Institute, Federal University of Rio Grande do Sul (UFRGS), Av. Bento Gonçalves, 9500 - Prédio 43126 - Sala 211, Caixa Postal 15001, Porto Alegre, RS 91501-970, Brazil

waste, taking into consideration the dimensions that it will acquire in the next years. It is also necessary to evaluate the risks of disposing the WEEE, which can generate environmental impacts [5], given that the waste contains hazardous materials that require special handling and can cause possible detrimental effects on human health. Moreover, recycling can recover reusable components and base materials such as copper [6], precious metals [7, 8], and reserves of carbon [9].

## Photovoltaic Modules

The composition of PV modules varies according to the technology used. The modules are basically a layer of a semiconductor material placed between tempered glass and/or glass or a polymer as back sheet. Lead, chromium, cadmium, and nickel are among the hazardous metals usually used [10]. Currently, silicon (Si)-based PV modules, such as single-crystalline Si (sc-Si), multicrystalline Si (mc-Si), and hydrogenated amorphous Si (a-Si) PV modules, are playing a vital role in the PV market [11]. A general quantification of the materials present in silicon-based PV modules is shown in Table 1.

Modules are encapsulated with various materials to protect the cells and the electrical connectors from the environment [14]—the most common being ethylene–vinyl acetate (EVA). The removal of these encapsulating materials is an important step in the recycling of PV modules [15] (Fig. 1).

Thermal and hydrometallurgical processes are prevalent in most of the PV recycling methods, and the encapsulating material can be removed with the aid of thermal decomposition and nitric acid [16]. Jung et al. [17] used a thermal treatment to decompose the EVA layer and to separate the different layers of solar panels. Doi et al. [18] used various organic solvents aiming to dissolve the EVA layer.

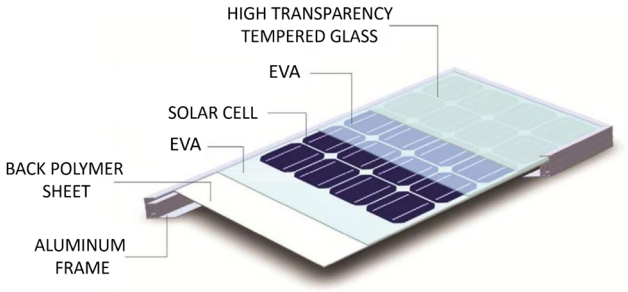


**Fig. 1** Arrangement of components in a typical silicon-based solar module. Adapted from [13] (Color figure online)

Radziemska et al. [19] used a thermal process to decompose the EVA, followed by a chemical treatment for the solar cell, which they refer to as a second primary step in PV modules' recycling. Kang et al. [20] employed a mixture of acid solvents in the process of etching Si solar panels. Zhang and Xu [21] used pyrolysis in a nitrogen atmosphere to remove the EVA layer, and recycle glass and gallium from thin-film solar modules. However, as shown in earlier studies [5], the use of mechanical processes, such as shredding/milling, and sieving, may assist in the recycling of PV panels and reduce the cost of recycling, given that these processes are able to concentrate metals in different fractions according to particle size. Moreover, mechanical processes may be used prior to the thermal and hydroprocesses as a pretreatment step that aids the following recycling steps and upgrades material content [22, 23].

## Electrostatic Separation

Electrostatic separation is frequently used in the separation of equipment containing copper, aluminum, and insulating materials, which is also the case of WEEE. It represents a

**Table 1** Typical composition of materials in a silicon-based photovoltaic module. Source: [5, 8, 12, 13]

| Material | Content/wt% | Purpose |
|---|---|---|
| Silicon | 2–3 | Photovoltaic effect |
| Glass | 69–75 | Module protection, allowing light to reach PV cell |
| Polymers (EVA, Tedlar) | 7 | Module protection, encapsulating PV cell, isolating module from surroundings |
| Copper | 0.6–1 | Current conductor |
| Silver | 0.006–0.06 | Current conductor |
| Aluminum | 10–20 | Module frame, p-doping silicon, current conductor |
| Boron | < 0.1 | p-doping of silicon |
| Phosphorus | < 0.1 | n-doping of silicon |
| Tin dioxide | < 0.1 | Anti-reflection (AR) coating |
| Lead | < 0.1 | Copper coating |
| Tin | < 0.1 | Copper coating |

modern and useful technology for the recycling of industrial waste materials [24, 25]. Electrostatic separation sorts substances with different electrical conductivities, which are typically charged before exposure to electrostatic and gravitational forces. In a roll-type separator (Fig. 2), the materials go through a grounded roller and are subjected to electric charge ionization from an electrode; conductive particles discharge due to physical contact with the roller, while nonconductive particles are attracted to the roller due to Coulomb forces. Thus, the particles are eventually separated due to the differences in conductivity and electrostatic properties [26].

Richard et al. [28] applied electrostatic separation to sort out granular metals and plastics from electric wire waste. Recently, the same authors evaluated the use of three different configuration of roll-type electrostatic separation in order to optimize the segregation of PVC (Polyvinyl chloride), aluminum and copper from electronic waste. The three configurations included the use of an (i) elliptical static electrode with corona effect, an (ii) s-shaped plate with plastic trap and (iii) an s-shaped plate with plastic trap and corona effect. They have found that the corona electrode (or ionizing electrode) is necessary for the separation of PVC and copper [29]. Veit et al. [30] also used this method to recover metals from circuit boards and concluded that the use of electrostatic separation was efficient in obtaining high concentrated fractions of metals, in particular, he was able to concentrate 50% of copper, 25% of tin, and 7% of lead. This method has been further improved by adding a second roll and creating a two-step process [31]. Electrostatic separation is considered an efficient low cost mechanical process that requires little energy in comparison to thermal processes [32] and does not generate byproduct effluents, unlike hydrometallurgical processes [33].

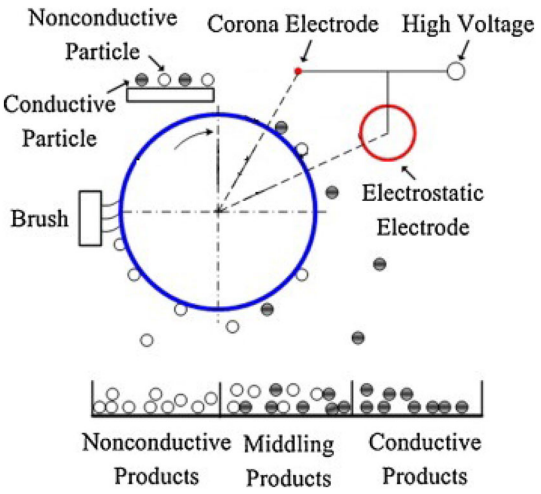


**Fig. 2** Diagram illustrating the electrostatic separation principle in a roll-type electrostatic separator. Adapted from [27] (Color figure online)

As demonstrated, thermal and hydrometallurgical methods are largely implemented in the recycling of waste PV and the combination of both is currently presenting optimal outputs [15, 19, 20]. The use of electrostatic separation in PV recycling has not yet been studied despite the great potential this method has in assisting the recycling through the segregation of different materials present in the modules. Moreover, the use of electrostatic separation could potentially reduce the cost of PV recycling, which is one of the biggest barriers keeping the recycling of WEEE from expanding [34]. Therefore, in this study, the use of electrostatic separation is assessed in order to segregate the main materials of PV panels.

## Materials and Methods

The objective of this study is to evaluate the use of electrostatic separation technique to segregate some of the main materials present in silicon-based photovoltaic modules: silver, copper, silicon, glass, and polymers from the back sheet and encapsulating material. The schematic diagram (Fig. 3) outlines the principle of investigations performed in this study.

The experiments were performed with five different crystalline silicon modules (c-Si modules). The aluminum frames were manually removed from all modules. The modules were then milled with a SRB 2305 knife mill (Rone, São Paulo, Brasil) with the experimental parameters based on previous works [8]. The milling was repeated four times, the first two using a screen with 4-mm openings and the second two using a screen with 2-mm openings; the output powder weighed approximately 5 kg.

The output powder was quartered and separated in 300-g samples. These samples were named F1, F2, F3, F4, F5, and F6. In the first part of the experiment, empirical studies were performed by attempting to separate the different materials from the sample by varying several parameters at random starting points. The equipment used for all the electrostatic separations was a MMPM-618C (Eriez, Erie, USA) high-tension roll separator (Fig. 4).

Visual inspection was adopted to determine the performance of a given parameter. A sample considered great would have the majority of polymers on output C, the majority of silicon on output B, and the majority of glass and metals in output A. The changeable parameters are listed in Table 2, which also presents the parameters that were fixed (pinned down) after repetitive attempts of separating the materials and observing the results.

It is important to notice that there are only three collection pans (Fig. 4—item 9): conductor, middling, and nonconductor: A, B, and C, respectively. Samples F1, F2, and F3 were used in the empirical study.

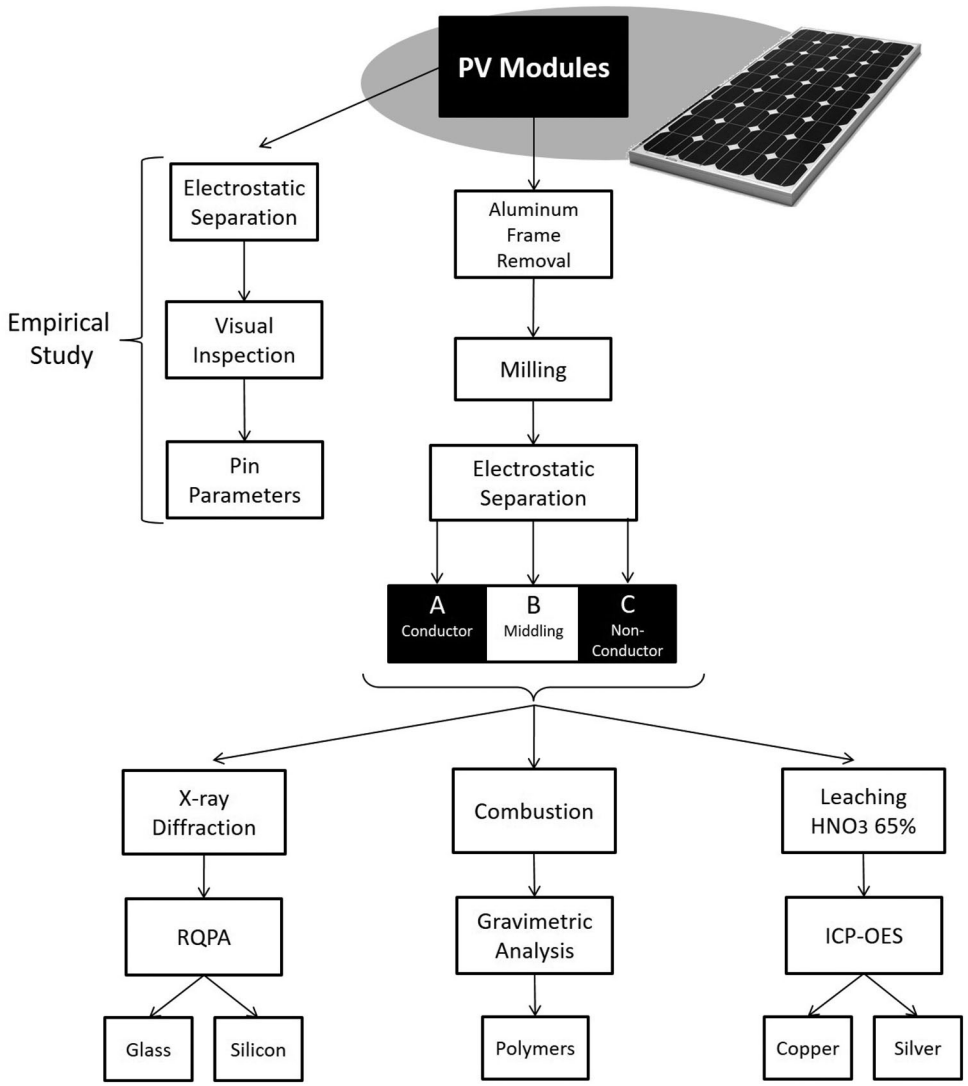


**Fig. 3** Schematic diagram illustrating the procedures used in this study.

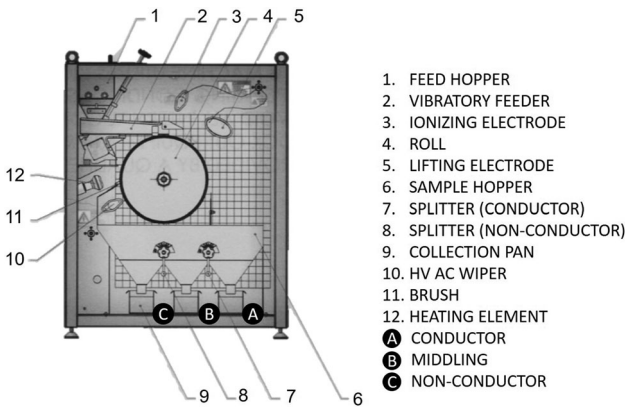


**Fig. 4** Schematic illustration of the electrostatic separator equipment setup. Adapted from [35]

The results obtained from the empirical study led to the restriction of the degrees of freedom related to the variables in the separation process. As a result, it was chosen to vary the electric potential difference and the rotation speed and keep the other parameters fixed. The electric potential difference (voltage hereafter) is given in volts and is the difference in electric potentials between wired electrodes (lifting and ionizing) and the roll (grounded). The selected voltages were 24 and 28 kV; the selected rotation speeds were 50, 65, and 80 RPM.

Each 300-g group (F4, F5, and F6) was quartered and separated in six 50-g samples—one for each combination of parameters. 50-g samples were chosen based on previous WEEE electrostatic separation studies [29]. The end result after electrostatic separation is a total of 18 samples (six combinations of parameters with output fractions A, B and C), which were replicated three times (F4, F5 and F6) for further statistical analyses. To evaluate the efficiency of each combination of voltage and rotation speed, a series of experiments were performed: First, each sample was leached in nitric acid (65% concentration) solution using a 10:1 liquid–solid ratio, under magnetic stirring, at room

**Table 2** Relationship between parameters and variation for the electrostatic separator used in this study

| Parameters | Variation | Position in Fig. 4 | Fixed? | Pinned at |
|---|---|---|---|---|
| Splitter angle (conductor) | [− 45° to + 45°] | 7 | Yes | 10° |
| Splitter angle (nonconductor) | [− 45° to + 45°] | 8 | Yes | 22° |
| Vibratory feeder speed | 0–100% | 2 | Yes | 25% |
| Preheating | 0–60 °C | 12 | Not used | Room temperature |
| Rotation speed | 0–300 RPM | 4 | No | – |
| Electric potential difference | 0–40 kV | 3, 4, 5 | No | – |
| Ionizing electrode position | Position in a 650 × 720 $mm^2$ area having the roll electrode on the center, *X* as the horizontal axis, and *Y* as the vertical | 3 | Yes | *x* [90;240]<br>*y* [110;260] |
| Lifting electrode position | *X* = [− 200 to + 450 mm]<br>*Y* = [− 450 to + 270 mm] | 5 | Yes | *x* [255; 450]<br>*y* [95; 160] |
| Brush position | | 11 | Yes | *x* [– 200; – 170<br>*y* [– 70; 35]] |

temperature. The solid part from the leaching was filtered, rinsed, dried, and put aside. The solutions containing the leached metals were analyzed by inductively coupled plasma optical emission spectroscopy (ICP-OES) to determine the amount of silver and copper in each sample. The equipment used was a 5110 ICP-OES (Agilent Technologies, California, USA). The filter residue was then weighed and placed in a crucible, which was placed inside a furnace in order to eliminate the polymers in each sample. The dwell temperature was set to 500 °C based on previous works [15]. The heating ramp was 15 °C/min and the dwell time was 5 h per sample. The samples were weighed again and the mass difference was assumed to be the mass of the polymeric fraction contained in each sample.

Finally, the samples were milled in an alumina mortar and sieved through a mesh 400 sieve (37 μm). Each sample was weighted and analyzed by X-ray diffraction (XRD) using a Siemens (Bruker AXS—Germany) D-5000 diffractometer with Cu Kα1,2 radiation (1.54178 Å) and equipped with curved graphite monochromator in the secondary beam. The data were collected in the Bragg–Brentano ($\theta/\theta$) geometry between 10 and 75° ($2\theta$) in 0.05° steps, at 1 s/step using a 1° divergence, and anti-scattering slits, and a detector slit of 0.6 mm.

After initial analysis, an internal standard of hexagonal (P63 mc) ZnO (99.9%) was added to the sample. The internal standard was added so that it would represent 10% in weight of the sample. For Rietveld quantitative phase analysis (RQPA), the same angular interval was analyzed in 0.02° steps, at 15 s/step using a 1° divergence and anti-scattering slits, and a detector slit of 0.2 mm. The X-ray tube was operated at 40 kV and 40 mA [36]. The Si and ZnO contents were determined by RQPA using a free-code software MAUD (Materials Analysis Using Diffraction [37]. After RQPA, the amorphous content was determined using Eq. (1).

$$A = \frac{1 - \frac{Ws}{Rs}}{100 - Ws} \times 10^4\%, \quad (1)$$

where (%) is the weighted concentration of the internal standard and (%) is the Rietveld-analyzed concentration of the internal standard [36, 38]. The amorphous phase is assumed to be glass, while the crystalline phase is assumed to be silicon.

The optimal parameter to separate materials from waste PV modules is given by the analysis of the distribution of material in A, B and C (Fig. 4). In the interest of evaluating the effectiveness of electrostatic separation and the optimal parameter combination, a variance analysis was performed, and p-values were generated to determine significance for a confidence level of 95% ($\alpha = 0.05$). The variance analysis was performed for the silver, copper, and polymer separation. Because of the cost of XRD and RQPA analysis, it was not possible to perform a variance analysis for glass and silicon as this requires replicated measurements.

## Results

In the first part of the experiment, an empirical study was carried out in order to restrain the degrees of freedom related to the electrostatic separation. Initially, all parameters varied, and the output of each combination was analyzed by visual inspection. As a result, the fixed parameters were the two splitter angles, the vibratory feeder speed, and the position of the ionizing electrode, the brush and the lifting electrode. The visual inspection

revealed a clear separation among the main materials present in waste PV modules. As can be seen in Fig. 5, the nonconductor fraction (C) contains mostly polymers (white particles), the middling fraction (B) contains mostly silicon (gray and blackish particles) and the conductor fraction (A) mostly contains glass. Although glass is an electrical insulating material [39], its particles fall into the first pan along with the metals (conductive fraction: A). This may be due to particles being too heavy (speed gained during rotation is superior to the electrostatic forces acting) and/or due to the influence of metallic particles, which can attach to the glass particles through the encapsulating material.

The following experiments determined which would be the values for voltage and rotation speed used in this study. Rotation speed varied from 15 to 85 RPM and the voltage from 10 to 30 kV (voltages higher than 30 kV were not tested because electrical discharges start taking place at this point). Each output was evaluated by visual inspection and classified as poor, fair, good, and great. The results are displayed in Table 3.

Table 3 shows two results classified as "great": 28 kV with 30 RPM and 28 kV with 55 RPM. The table also shows that the best results are obtained with a voltage of 24 kV or higher and a rotation speed of 30 or higher. Thus, two voltage values (24 and 28 kV) and three rotation speed values (50, 65, and 80 RPM) were chosen to quantitatively evaluate the separation of materials from waste PV modules.

The distributions of silver and copper for each parameter combination obtained by ICP-OES are displayed in Figs. 6 and 7, respectively.

Both Figs. 6 and 7 indicate that metals tend to concentrate in the first fraction (A), followed by the second and third (B and C). It should be highlighted that the metal concentration in C is around 5% on average. Therefore, the electrostatic separation concentrates about 95% of silver and copper in fractions A and B. The copper did not follow this distribution for the combination 24 kV-65 RPM nor 28 kV-50 RPM. While 100% of separation was not achieved at this point, these results indicate that electrostatic separation is able to separate the metal content from photovoltaic waste, but also show that there is no significant difference between the treatments (combinations of parameters) tested in this study in regard to metal separation. Figure 8 supports the statement that there is a significant difference between the three fraction outputs. The detailed distributions of silver and copper are available in Supplementary Tables 1 and 2, respectively.

The polymer distribution was measured by gravimetric analysis. The mass differences before and after combustion are assumed to be the mass of polymers present in a certain sample. The variance analysis for the polymer distribution is shown in Fig. 9, and the average polymer distributions in pans A, B, and C are displayed in Fig. 10. Figure 9 indicates that the combinations of parameters tested for the electrostatic separation do not differ significantly among each other.

Moreover, Fig. 10 shows that it was not possible to segregate the polymers in any of the separation pans. It has been reported that photovoltaic panels may have polyvinyl chloride (PVC) in its substrate [15]. Richard et al. [29] have stated that the use of a reverse s-shaped electrode assists in the separation of PVC by this method. The presence of PVC in waste PV may have influenced the separation process. The detailed distribution of polymers is available in supplementary Table 3.

The silicon and glass distributions were measured by XRD with Rietveld's refinement. The amorphous phase was assumed to be glass, while the crystalline phase was assumed to be silicon. The distributions of glass and silicon in the three pans for all tested parameters are displayed Fig. 10, while the uncertainties associated with the Rietveld's refinement for the analysis of this study are presented in Supplementary Table 6.

Figure 10 suggests that glass tends to concentrate in the first fraction (conductor: A) as predicted from the empirical study. Moreover, for a significance of $p < 0.001$, fraction sA and B concentrate approximately 95% of the glass. A similar behavior is found with the silicon, given it concentrated mainly in A, followed by B and C. The standard

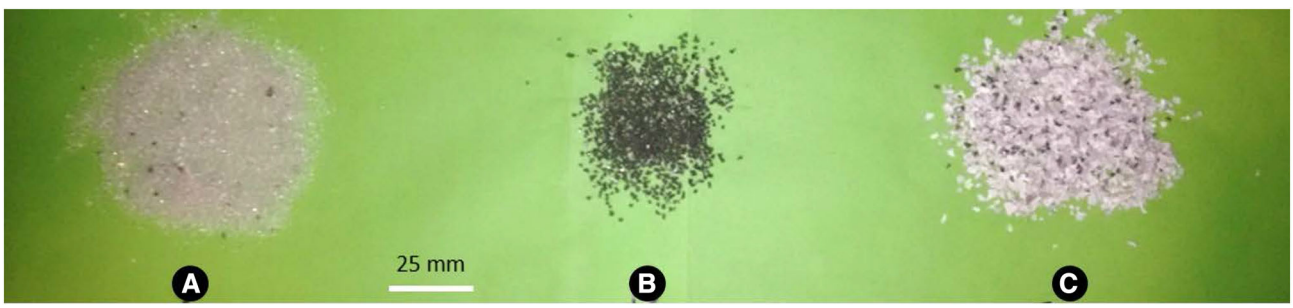


**Fig. 5** Visual analysis comparing the three different outputs from the electrostatic separation during the empirical study. Conductor (**a**), middling (**b**) and nonconductor (**c**) (Color figure online)

**Table 3** Qualitative results from empirical study to determine key values of voltage and rotation speed

| Voltage (kV) | Rotation speed (RPM) | Classification | Comment |
|---|---|---|---|
| 10 | 15 | Poor | No separation. All in B |
| 10 | 30 | Poor | No separation. All in B |
| 10 | 45 | Poor | Little improvement, glass in A, the rest in the B |
| 10 | 55 | Poor | No separation. All in C |
| 10 | 85 | Poor | No separation. All in C |
| 12 | 30 | Poor | Almost all sample in B |
| 14 | 30 | Fair | Glass in A, the rest in B |
| 16 | 30 | Fair | Improvement. Some polymer in C |
| 18 | 30 | Fair | Improvement. Most of it still in B |
| 20 | 30 | Fair | Improvement. Better distribution among the three pans |
| 22 | 30 | Fair | Same as previous |
| 24 | 30 | Good | Most of the glass in A, polymers in C |
| 26 | 30 | Good | Little improvement from previous |
| 28 | 30 | Great | Most of the glass in A, most of the polymer in C, silicon, and polymers mixed in B |
| 30 | 30 | – | Electrical discharge (arcing) observed at this voltage |
| 28 | 15 | Good | Nonconductive material concentrated in C |
| 28 | 45 | Good | Most of the glass in A, most of the polymer in C, silicon in B and C |
| 28 | 55 | Great | Similar to previous, but most of the silicon in B |
| 28 | 70 | Good | Similar to previous, but silicon did not concentrate in B as much |

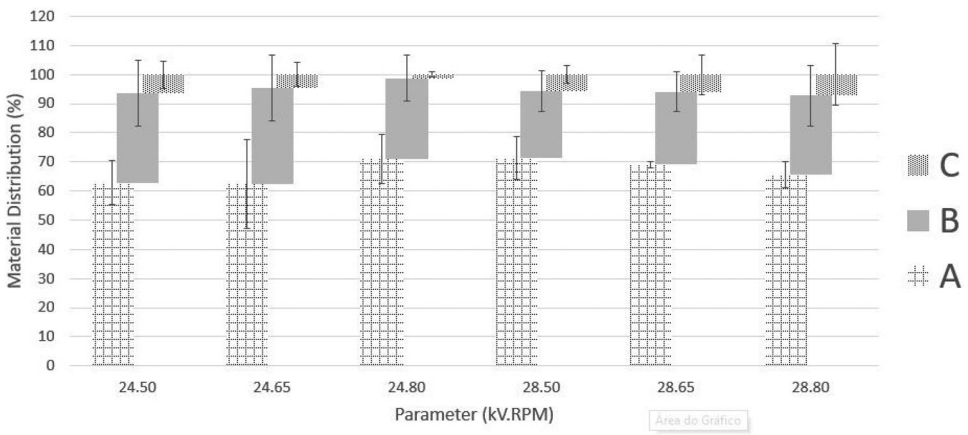


**Fig. 6** Average distribution of silver in each fraction for a given combination of chosen parameters ($p$-values for A, B, and C distribution are 0.662, 0.789, and 0.856, respectively). There were three replicates per parameter

deviations suggest that it is possible to concentrate silicon in the second fraction (middling) with the appropriate combination of parameters. The influences of each combination of parameters on the material distribution for glass and silicon are displayed in Figs. 11 and 12.

The detailed distributions of glass and silicon are available in Supplementary Tables 4 and 5, respectively.

Figure 11 shows that for all the combination of parameters tested, glass mostly stays in the first fraction. This is probably due to its weight, i.e., most of the glass particles have a mass such that the gravitational force has a greater influence than the electrostatic force from the process. The smaller glass particles are the ones found in the last fraction (nonconductor: C). As for the silicon, Fig. 12 shows that for different combination of parameters (particularly for 24.50 and 28.80), it is possible to concentrate this material in the second fraction (middling: B), but for the combinations of this study, it tends to remain on the first fraction (conductor: A). Silicon particles in PV waste are distributed in fine particles that can remain attached to particles of other material. This may affect the distribution of silicon particles during the electrostatic separation. The assessment of the different combination of parameters is limited given that a single analysis for each combination of parameters was made for glass and silicon. Therefore, a statistical analysis is not possible for these given parameters. Moreover, the mass distributions in the three pans as a function of the tested parameters are shown in Supplementary Table 7.

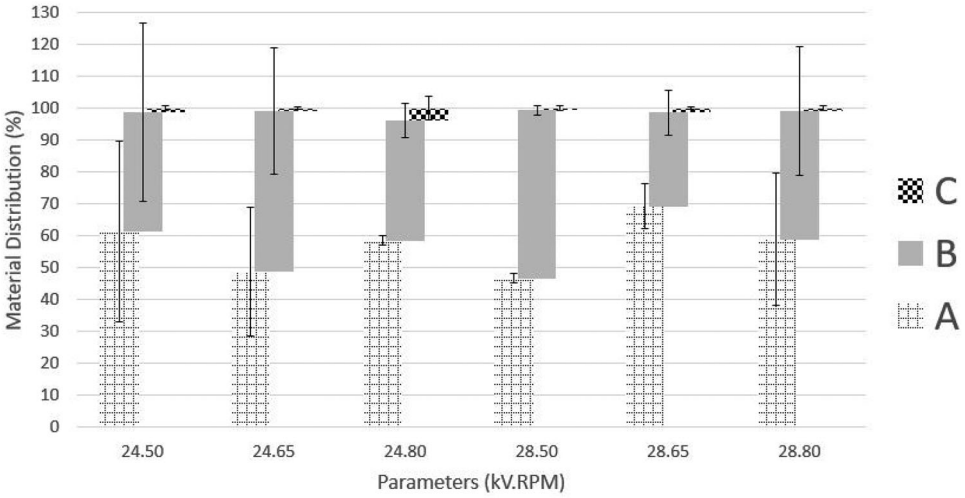


**Fig. 7** Average distribution of copper in each fraction for a given combination of chosen parameters ($p$-values for A, B, and C distribution are 0.606, 0.552, and 0.209, respectively). There were three replicates per parameter

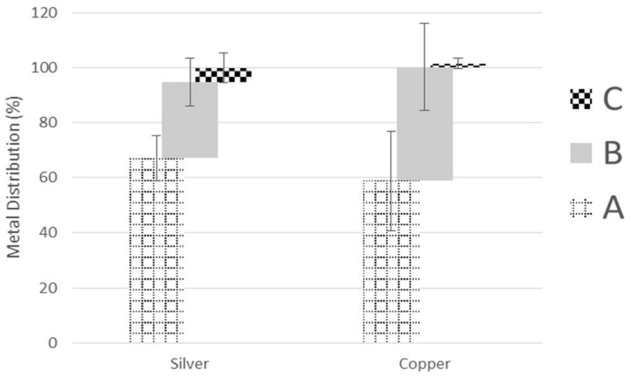


**Fig. 8** Electrostatic separation's influence on silver and copper content distributions ($p$ value for silver and copper distribution is $< 0.001$)

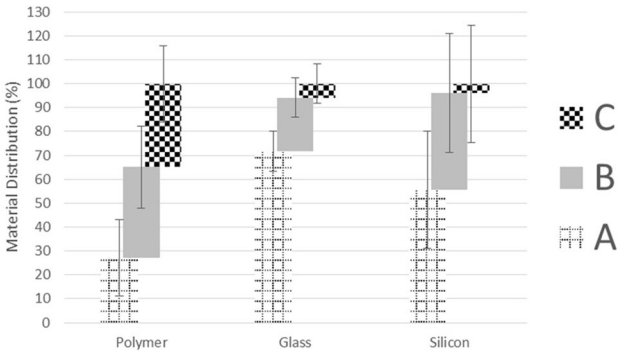


**Fig. 10** Electrostatic separation's influence on polymer, glass, and silicon content distributions ($p$-values of polymer, glass, and silicon distribution are 0.146, $< 0.001$, and $< 0.001$, respectively)

**Fig. 9** Average distribution of polymer in each fraction for a given combination of chosen parameters ($p$-values for A, B, and C distributions are 0.834, 0.051, and 0.933, respectively). There were three replicates per parameter

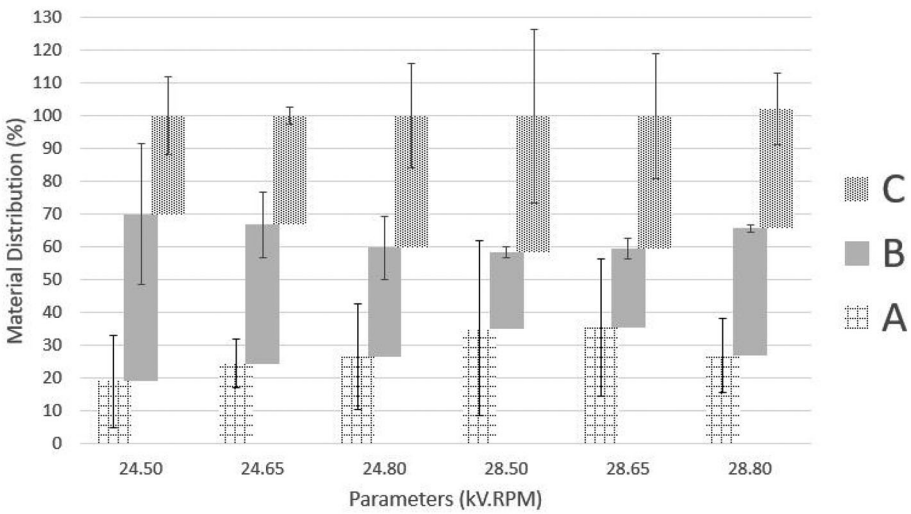

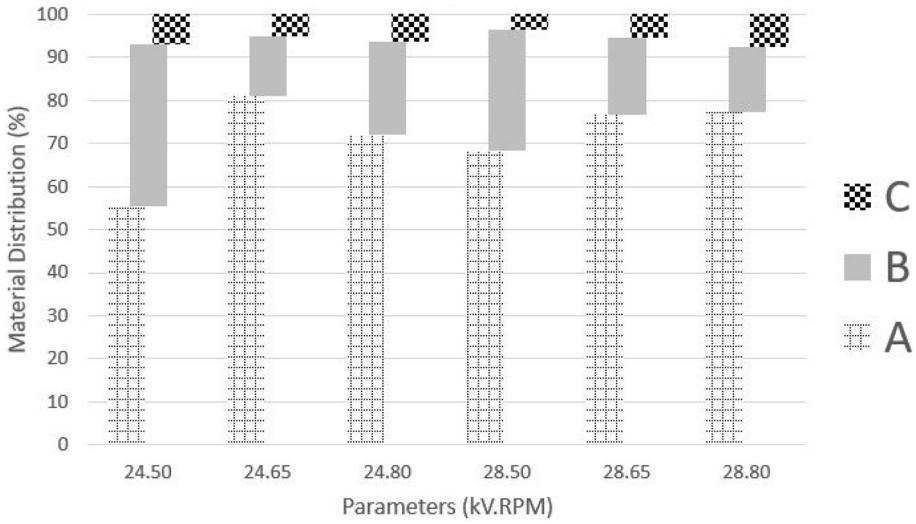


**Fig. 11** Distribution of glass in each fraction for a given combination of chosen parameters

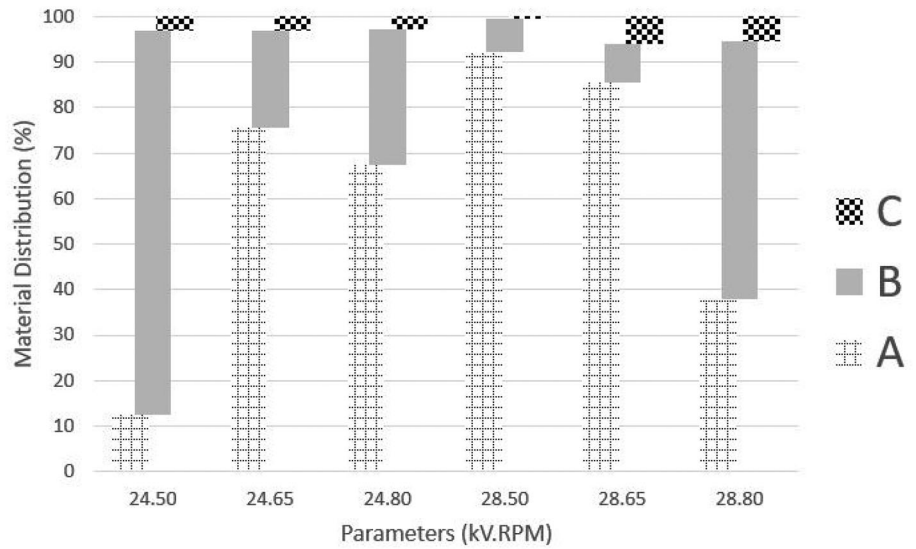


**Fig. 12** Distribution of silicon in each fraction for a given combination of chosen parameters

## Conclusions

The key conclusions from this study are as follows:

- Electrostatic separation is able to segregate the metallic fraction of waste photovoltaic panels. Metals tend to concentrate in the first separation fraction (conductor). About 95% of the metals in waste silicon photovoltaic modules concentrate in output pans A and B (conductor and middling, respectively) combined.
- The studied combination of parameters have no statistical differences among each other for the separation of metals. The influence of the parameters was not significant for either silver or copper.
- Electrostatic separation was not able to concentrate the polymers present in photovoltaic panels. The presence of PVC as one of the polymers present in photovoltaic panels may have contributed to the failure of the electrostatic separation method [15, 29].
- The studied combination of parameters have no statistical difference among each other for the separation of polymers. The influence of the parameters was not significant.
- The glass present in waste PV tends to concentrate in the conductive fraction, followed by the middling and nonconductor ($p < 0.001$).
- For the majority of tested combination of parameters, silicon tends to concentrate in the first output fraction (conductor). However, it was shown that it is possible to concentrate silicon in the second output fraction (middling) by varying the parameters.
- Among the tested combination of parameters (24 kV.50RPM; 24 kV.65RPM; 24 kV.80RPM; 28 kV.50RPM; 28 kV.65RPM; 28 kV.80RPM), it is

not possible to determine the optimal combination of parameters for separating metals and polymers from photovoltaic modules at this stage.
- Electrostatic separation has an influence in most of the materials present in waste silicon photovoltaics. This process may assist in the recycling of waste PV.

This study can be improved by means of samples with higher masses for each parameter combination (e.g., 300 g), by evaluating the separation at a lower rotation speed (e.g., 20, 30, and 40 RPM); by using a reversed s-shaped plate so that materials such as PVC are more influenced by the separation (as stated by Richard et al. [29]); and by heating the samples before the separation to reduce the humidity. The improvement of this study is encouraged by the results observed. Electrostatic separation can assist in the recycling of waste photovoltaics, but the parameters for an optimal separation are still uncertain.

**Acknowledgements** The authors are grateful to Capes, CNPq, FINEP, and FAPERGS (Brazil) for their financial support.

## References

1. Zuser A, Rechberger H (2011) Considerations of resource availability in technology development strategies: the case study of photovoltaics. Resour Conserv Recycl 56:56–65. https://doi.org/10.1016/j.resconrec.2011.09.004
2. Kalogirou S (2009) Solar energy engineering: processes and systems, 1st edn. Elsevier, San Diego
3. Tao J, Yu S (2015) Review on feasible recycling pathways and technologies of solar photovoltaic modules. Sol Energy Mater Sol Cells 141:108–124. https://doi.org/10.1016/j.solmat.2015.05.005
4. Weckend S, Wade A, Heath G (2016) End-of-life management: solar photovoltaic panels. National Renewable Energy Laboratory (NREL), Golden
5. Dias PR, Benevit MG, Veit HM (2016) Photovoltaic solar panels of crystalline silicon: characterization and separation. Waste Manag Res 34:235–245
6. Robinson BH (2009) E-waste: an assessment of global production and environmental impacts. Sci Total Environ 408:183–191. https://doi.org/10.1016/j.scitotenv.2009.09.044
7. Tickner J, Rajarao R, Lovric B et al (2016) Measurement of gold and other metals in electronic and automotive waste using gamma activation analysis. J Sustain Metall 2:296–303. https://doi.org/10.1007/s40831-016-0051-y
8. Dias P, Javimczik S, Benevit M et al (2016) Recycling WEEE: extraction and concentration of silver from waste crystalline silicon photovoltaic modules. Waste Manag 57:220–225. https://doi.org/10.1016/j.wasman.2016.03.016
9. Sahajwalla V, Cayumil R, Khanna R et al (2015) Recycling polymer-rich waste printed circuit boards at high temperatures: recovery of value-added carbon resources. J Sustain Metall 1:75–84. https://doi.org/10.1007/s40831-014-0002-4
10. Tammaro M, Salluzzo A, Rimauro J et al (2016) Experimental investigation to evaluate the potential environmental hazards of photovoltaic panels. J Hazard Mater 306:395–405. https://doi.org/10.1016/j.jhazmat.2015.12.018
11. Chantana J, Kamei A, Minemoto T (2017) Influences of environmental factors on Si-based photovoltaic modules after longtime outdoor exposure by multiple regression analysis. Renew Energy 101:10–15. https://doi.org/10.1016/j.renene.2016.08.037
12. Radziemska E (2014) Recycling of photovoltaic solar cells and modules-the state-of-art. LAP LAMBERT Academic Publishing, Saarbrucken
13. Pinho JT, Galdino MA (2014) Engineering manual for photovoltaic systems retrieved from Rio de Janeiro: CEPEL—CRESESB. Manual de engenharia para sistemas fotovoltaicos
14. Hansen AD, Sorensen P, Hansen LH, Bindner H (2000) Models for a stand-alone PV system. Riso National Laboratory, Roskilde
15. Dias P, Javimczik S, Benevit M, Veit H (2016) Recycling WEEE: polymer characterization and pyrolysis study for waste of crystalline silicon photovoltaic modules. Waste Manag 60:716–722. https://doi.org/10.1016/j.wasman.2016.08.036
16. Bruton TM (1994) Re-cycling of high value, high energy content components of silicon PV modules. In: Proceedings of 12th EC-PVSEC, pp 459–463
17. Jung B, Park J, Seo D, Park N (2016) Sustainable system for raw-metal recovery from crystalline silicon solar panels: from noble-metal extraction to lead removal. ACS Sustain Chem Eng 4:4079–4083. https://doi.org/10.1021/acssuschemeng.6b00894
18. Doi T, Tsuda I, Unagida H et al (2001) Experimental study on PV module recycling with organic solvent method. Sol Energy Mater Sol Cells 67:397–403
19. Klugmann-Radziemska E, Ostrowski P (2010) Chemical treatment of crystalline silicon solar cells as a method of recovering pure silicon from photovoltaic modules. Renew Energy 35:1751–1759. https://doi.org/10.1016/j.renene.2009.11.031
20. Kang S, Yoo S, Lee J et al (2012) Experimental investigations for recycling of silicon and glass from waste photovoltaic modules. Renew Energy 47:152–159. https://doi.org/10.1016/j.renene.2012.04.030
21. Zhang L, Xu Z (2016) Separating and recycling plastic, glass, and gallium from waste solar cell modules by nitrogen pyrolysis and vacuum decomposition. Environ Sci Technol 50:9242–9250. https://doi.org/10.1021/acs.est.6b01253
22. Cui J, Zhang L (2008) Metallurgical recovery of metals from electronic waste: a review. J Hazard Mater 158:228–256. https://doi.org/10.1016/j.jhazmat.2008.02.001
23. Dias P, Machado A, Huda N, Bernardes AM (2018) Waste electric and electronic equipment (WEEE) management: a study on the Brazilian recycling routes. J Clean Prod 174:7–16. https://doi.org/10.1016/j.jclepro.2017.10.219
24. Tilmatine A, Medles K, Bendimerad S-E et al (2009) Electrostatic separators of particles: application to plastic/metal, metal/metal and plastic/plastic mixtures. Waste Manag 29:228–232. https://doi.org/10.1016/j.wasman.2008.06.008
25. Cui J, Forssberg E (2003) Mechanical recycling of waste electric and electronic equipment: a review. J Hazard Mater 99:243–263. https://doi.org/10.1016/S0304-3894(03)00061-X
26. Lai KC, Lim SK, Teh PC, Yeap KH (2016) Modeling electrostatic separation process using artificial neural network (ANN). Procedia Comput Sci 91:372–381. https://doi.org/10.1016/j.procs.2016.07.099
27. Wu J, Qin Y, Zhou Q, Xu Z (2009) Impact of nonconductive powder on electrostatic separation for recycling crushed waste printed circuit board. J Hazard Mater 164:1352–1358. https://doi.org/10.1016/j.jhazmat.2008.09.061
28. Richard G, Touhami S, Zeghloul T, Dascalescu L (2016) Optimization of metals and plastics recovery from electric cable wastes using a plate-type electrostatic separator. Waste Manag 60:112–122. https://doi.org/10.1016/j.wasman.2016.06.036
29. Richard G, Salama A, Medles K et al (2017) Comparative study of three high-voltage electrode configurations for the electrostatic

separation of aluminum, copper and PVC from granular WEEE. J Electrost 88:29–34. https://doi.org/10.1016/j.elstat.2016.12.022
30. Veit HM, Diehl TR, Salami AP et al (2005) Utilization of magnetic and electrostatic separation in the recycling of printed circuit boards scrap. Waste Manag 25:67–74. https://doi.org/10.1016/j.wasman.2004.09.009
31. Jiang W, Jia L, Zhen-ming X (2009) A new two-roll electrostatic separator for recycling of metals and nonmetals from waste printed circuit board. J Hazard Mater 161:257–262. https://doi.org/10.1016/j.jhazmat.2008.03.088
32. Kaya M (2016) Recovery of metals and nonmetals from electronic waste by physical and chemical recycling processes. Waste Manag 57:64–90. https://doi.org/10.1016/j.wasman.2016.08.004
33. Awasthi AK, Li J (2017) An overview of the potential of eco-friendly hybrid strategy for metal recycling from WEEE. Resour Conserv Recycl 126:228–239. https://doi.org/10.1016/j.resconrec.2017.07.014
34. Sahajwalla V, Pahlevani F, Maroufi S, Rajarao R (2016) Green manufacturing: a key to innovation economy. J Sustain Metall 2:273–275. https://doi.org/10.1007/s40831-016-0087-z
35. ERIEZ (2013) MMPM-618C Installation operation maintenance manual—laboratory electrostatic separator; high tension roll (HTR) separator
36. De La Torre AG, Bruque S, Aranda MAG (2001) Rietveld quantitative amorphous content analysis. J Appl Crystallogr 34:196–202. https://doi.org/10.1107/S0021889801002485
37. Lutterotti L, Matthies S, Wenk H-R (1999) MAUD (material analysis using diffraction): a user friendly Java program for Rietveld texture analysis and more. In: Proceeding of the twelfth international conference on textures of materials (ICOTOM-12). NRC Research Press, Ottawa, p 1599
38. Young RA (1995) The Rietveld Method. Oxford University Press, Oxford
39. Bansal NP, Doremus RH (2013) Handbook of glass properties. Elsevier, New York